# Constraint of soil moisture on $CO_2$ efflux from tundra lichen, moss, and tussock in Council, Alaska, using a hierarchical Bayesian model

**Yongwon Kim[1]*, Kazuya Nishina[2], Namyi Chae[3], Sangjong Park[4], Youngjun Yoon[5], and Bangyong Lee[5]**

[1]{International Arctic Research Center, University of Alaska Fairbanks, AK 99775-7335, USA}

[2]{Center for Regional Environmental Research, National Institute for Environmental Studies, Tsukuba, 305-8506, Japan}

[3]{Civil and Environmental Engineering, Yonsei University, Seoul 120-749, Korea}

[4]{Division of Climate Change, Korea Polar Research Institute (KOPRI), Incheon 406-840, Korea}

[5]{Arctic Research Center, Korea Polar Research Institute (KOPRI), Incheon 406-840, Korea}

* Correspondence to: Yongwon Kim (kimyw@iarc.uaf.edu)

Key words: $CO_2$ efflux, Soil moisture and Temperature, Thaw depth, Lichen, Moss, Tussock tundra, Bayesian model

Running title: Constraint of soil moisture on $CO_2$ efflux in tundra ecosystem

## Abstract

The tundra ecosystem is quite vulnerable to drastic climate change in the Arctic, and the quantification of carbon dynamics is of significant importance in response to thawing permafrost, changes to the snow-covered period and snow and shrub community extent, and the decline of sea ice in the Arctic. Here, $CO_2$ efflux measurements using a manual chamber system within a 40 m × 40 m (5-m interval; 81 total points) plot were conducted within dominant tundra vegetation on the Seward Peninsula of Alaska, during the growing seasons of 2011 and 2012, for the assessment of driving parameters of $CO_2$ efflux. We applied a hierarchical Bayesian (HB) model—a function of soil temperature, soil moisture, vegetation type, and thaw depth—to quantify the effects of environmental factors on $CO_2$ efflux, and to estimate growing season $CO_2$ emission. Our results showed that average $CO_2$ efflux in 2011 is 1.4 times higher than in 2012, resulting from the distinct difference in soil moisture between the two years. Tussock-dominated $CO_2$ efflux is 1.4 to 2.3 times higher than those measured in lichen and moss communities, reflecting tussock as a significant $CO_2$ source in the Arctic, with wide area distribution on a circumpolar scale. $CO_2$ efflux followed soil temperature nearly exponentially from both the observed data and the posterior medians of the HB model. This reveals that soil temperature regulates the seasonal variation of $CO_2$ efflux and that soil moisture contributes to the interannual variation of $CO_2$ efflux for the two growing seasons in question. Obvious changes in soil moisture during the growing seasons of 2011 and 2012 resulted in an explicit difference between $CO_2$ effluxes—742 and 539 $gCO_2\,m^{-2}\,period^{-1}$ for 2011 and 2012, respectively, suggesting the 2012 $CO_2$ emission rate was constrained by 27 % (95 % credible interval: 17-36 %) compared to 2011, due to higher soil moisture from severe rain. The estimated growing season $CO_2$ emission rate ranged from 0.86 in 2012 to 1.20 $MgCO_2$ in 2011 within a 40 m × 40 m plot, corresponding to 86 % and 80 % of annual $CO_2$ emission rates within the Alaska western tundra ecosystem, estimated from the temperature dependence of $CO_2$ efflux. Therefore, this HB model can be readily applied to observed $CO_2$ efflux, as it demands only four environmental factors and can also be effective for quantitatively assessing the driving parameters of $CO_2$ efflux.

## 1. Introduction

Carbon dioxide ($CO_2$) efflux from the soil surface to the atmosphere is important for estimating regional and global carbon budgets (Schlesinger and Andrews, 2000; Bond-Lamberty and Thomson, 2010), as well as being susceptible to increasing air temperature (Bond-Lamberty and Thomson, 2010), the degradation of permafrost (Schuur et al., 2009; Jensen et al., 2014), and the expansion of the shrub community (Sturm et al., 2005). All of which suggests alteration of the terrestrial carbon cycle in response to drastic climate change in the Arctic (ACIA, 2004).

The tundra ecosystem of Alaska has received increased attention for the enhanced greening in abundant Arctic coastal shrubs that has come with the decline of sea ice (Bhatt et al., 2010; 2013; Post et al., 2013), the shortened snow-covered period (Hinzman et al. 2005), thawing permafrost, and shrinking ponds and lakes (Romanovsky et al. 2002; Yoshikawa and Hinzman, 2003; Hinzman et al. 2005; Smith et al. 2005)—all reflecting the changes in terrestrial carbon and water cycles (Davidson et al., 1998; Oechel et al. 2000; Michaelson and Ping, 2003; ACIA, 2004; Oberbauer et al. 2007; Walter et al. 2007; Koven et al. 2011). Recently, Jensen et al. (2014) found a distinct difference in $CO_2$ efflux from undisturbed tundra during 2011 and 2012, resulting from greater rainfall in the growing season of 2012. This suggests that higher soil moisture from rainfall is a suppressant factor for soil-produced $CO_2$ emitted to the atmosphere (Davidson et al., 1998; Oberbauer et al. 2007), decreasing $CO_2$ emission by 43 % (Jensen et al., 2014). Davidson et al. (1998) reported that $CO_2$ efflux increased with soil moisture from 0 to 0.2 $m^3$ $m^{-3}$, steadily decreasing after with increasing soil moisture content beyond 0.2 $m^3$ $m^{-3}$. Hence, $CO_2$ efflux magnitude depends profoundly on the extent of soil moisture. Further, soil temperature is well known as a significant factor for regulating $CO_2$ efflux in worldwide terrestrial ecosystems, as reported by many researchers (Davidson et al., 1998; Xu and Qi, 2001; Davidson and Janssens, 2006; Rayment and Jarvis, 2000; Kim et al., 2007, 2013; Jensen et al., 2014). $Q_{10}$ value, which is a measure of the change in reaction rate at intervals of 10 °C (Lloyd and Taylor, 1994), has been effectively used to evaluate the temperature sensitivity of soil microbial activity as an exponential function (Davidson et al., 1998; Xu and Qi, 2001; Monson et al., 2006; Bond-Lamberty and Thomson, 2010; Kim et al., 2013). For example, Monson et al.

(2006) estimated their highest $Q_{10}$ value, $1.25 \times 10^6$, as the beneath-snowpack soil temperature warmed from -3 to 0 °C in a high-elevation subalpine forest in Colorado, reflecting higher $CO_2$ production by beneath-snow microbes (such as snow molds) during the end winter and early spring season. In the well-drained soil of Zachenberg, Greenland, higher $CO_2$ concentration in frozen soil came from a soil-thawing spring burst event, related to the trapping of produced $CO_2$ during winter. Subsequently, there is a distinct difference in $Q_{10}$ value between above and below zero temperatures: $Q_{10}$ value below zero was 430, even when water content was 39 % (Elberling and Brandt, 2003). Therefore, soil temperature, which is an analogue of soil microbial activity under the assumption that soil moisture and substrate availability are not limiting factors, is the most important factor in producing $CO_2$ in the soil.

Monthly $CO_2$ efflux measured in the tundra ecosystem has been further recognized as having insufficient spatiotemporal resolution and efflux data representativeness from the conventional dynamic chamber method (Hutchinson and Livingston, 2002; Savage and Davidson, 2003). Oberbauer et al. (1992) developed a mathematical model, which proved that soil temperature and water table depth might be used as efficient predictors of ecosystem $CO_2$ efflux in the riparian tundra of the northern foothills of Alaska. In order to overcome the weakness of monthly $CO_2$ efflux measurement in the field, the hierarchical Bayesian (HB) model framework can be applied for estimation of $CO_2$ efflux from the tundra ecosystem, as in Clark (2005) and Nishina et al. (2009; 2012). Their results indicated that the HB model is an effective tool for the estimation of fluxes and evaluation of parameters with less bias. Lately, free software such as WinBUGS (http://www.mrc-bsu.ac.uk/bugs) has resulted in the availability of a HB model using the Markov Chain Monte Carlo (MCMC) method (Spiegelhalter and Best, 2000). Clark (2005) described that the HB model reveals complex nonlinear relationships between efflux and environmental factors.

In this study, we modeled observed $CO_2$ efflux using a HB model with four explanatory variables: soil temperature, soil moisture, vegetation types, and thaw depth, all under the assumption of the lognormal distribution. The HB model used in this study accommodated nonlinear relationships between efflux and environmental factors. Therefore, the objectives of this study are to 1) evaluate the effects of dominant plants on $CO_2$ efflux; 2) quantitatively assess

driving parameters of $CO_2$ efflux simulated by a hierarchical Bayesian (HB) model; and 3) estimate growing season $CO_2$ emission rate within a 40 m × 40 m plot in the western Alaska tundra ecosystem.

## 2. Materials and Methods

### 2.1. Study Site and Experimental Methods

The study site is dominantly covered by typical tussock tundra. This site is located at the community of Council (64°51'38.3" N; 163°42'39.7" W; 45 m.a.s.l.) on the Seward Peninsula, about 120 km northeast of Nome, Alaska. This site was selected for its relatively smooth transition from forest to tundra, with underlying discontinuous permafrost regime. The monthly average air temperature of 1.2 °C at the Nome airport from 1971 to 2010 ranged from -10.5 °C in January to 14.6 °C in July. Annual average precipitation was 427 mm, including snowfall (Western Regional Climate Center). During the growing seasons (June to September) of 2011 and 2012, average ambient temperature and precipitation were 8.9 ± 1.0 °C (CV, coefficient of variance: 12 %) and 285 mm, and 8.5 ± 2.8 °C (CV: 33 %) and 380 mm, respectively, as shown in Figure 1. Precipitation in July-August of 2011 and 2012 were 231 and 299 mm, respectively, corresponding to 81 and 79 % of growing season precipitation. Under heavy precipitation in early July of 2011, $CO_2$ efflux measurement could not be conducted, unfortunately, due to underestimation of $CO_2$ efflux. The sampling periods were June 17-24, August 2-8, and September 9-15 for 2011, and June 20-29, July 14-21, August 11-18, and September 8-15 for 2012. The Alaska DOT (Department of Transportation) has maintained the access road from Nome to Council from late May to late September. Because this access road was closed during the snow-covered period (October to May), we could not conduct $CO_2$ efflux measurement during the non-growing season. The Council site has been managed by the WERC (Water Environmental Research Center) of UAF (University of Alaska Fairbanks) since 1999, for changes in permafrost and the water cycle (Yoshikawa and Hinzman, 2003).

This study determined $CO_2$ efflux and environmental factors in lichen-, moss-, and tussock-dominant tundra microsites within a 40 m × 40 m plot (5-m interval; 81 points) at this

site during the growing seasons of 2011 and 2012. Our plot was established for better understanding of spatiotemporal variations of $CO_2$ efflux and environmental data. Within the 81-point area, on-ground dominant plants are lichen (*Cladonia mitis, Cladonia crispata,* and *Cladonia stellaris*); moss, such as sphagnum (*Sphagnum magellanicum*, *Sphagnum angustifolium,* and *Sphagnum fuscum*) and others (*Polytricum* spp., *Thuidium abietinum*, and *Calliergon* spp.); and cotton grass tussock tundra (*Eriophorum vaginatum*). Dominant lichen, moss, and tussock tundra were occupied the plot at 27, 53, and 20 % within the plot, respectively.

Soil temperatures were taken at 5 and 10 cm below the surface using a portable thermometer with two probes (Model 8402-20, Cole-Palmer, USA), and soil moisture was measured at each point with a portable soil-moisture logger (HH2, Delta-T Devices, UK) with sensor (ML2, Delta-T Devices, UK). Thaw depth was measured with a fiberglass tile probe (1.5 m long), and pH with a waterproof meter (IQ 160, Ben Meadows, USA) in September 2011, for soil characteristics. A one- or two-way ANOVA (95 % confidence level) and data regression analysis using Microsoft Excel Data Analysis software were performed.

### 2.2. Estimation of $CO_2$ Efflux

Our dynamic $CO_2$ efflux-measuring system was portable, convenient, and capable of calculating efflux *in-situ*. The 81-cylinder chamber base (30-cm dia., 40-cm height) was fixed to the surface at each point. This system consisted of a transparent-material chamber lid (35-cm dia., 0.3-cm thickness) with input and output urethane tubing (6 mm OD; 4 mm ID) and a pressure vent, a commercial pump (CM-15-12, Enomoto Micro Pump Co., Ltd., Japan), an NDIR $CO_2$ analyzer (Licor-820, LICOR Inc., USA), a commercial 12-V battery, and a laptop computer for efflux calculation (Kim et al., 2013). This system is similar to the manual system by Savage and Davidson (2003; see Figure 1). To minimize the effect of pressure inside the chamber, the flow rate of the pump was maintained at 0.5 $Lmin^{-1}$, due to under/overestimation of $CO_2$ efflux by under- or over-pressurization of the chamber used and caused by flow restrictions in air circulation design (Davidson et al., 2002). Efflux-measuring time was on a 5-10 minute interval, depending on weather and soil surface conditions. For tussock $CO_2$ efflux estimates, the surface area was variable and dependent on height; average tussock height in this case was 18.7 ± 5.1 cm

(CV: 27 %).

Efflux was calculated from the following equation, as described by Kim et al., (2013):

$$F_{CO2} = \rho_a \times (\triangle C/\triangle t) \times (V/A), \quad (1)$$

where $F_{CO2}$ represents measured soil $CO_2$ efflux (g $CO_2$ $m^{-2}$ $min^{-1}$), $\rho_a$ is the molar density of dry air ($molm^{-3}$), $\triangle C$ (ppmv) is the change in $CO_2$ concentration during measuring time ($\triangle t$, 5 to 10-min), $V$ is chamber volume, and $A$ is surface area (cross section = 0.070 $m^2$). The height of each chamber was also measured alongside the chamber to allow calculation of the efflux.

To assess the response of temperature dependence on $CO_2$ efflux, the relationship was plotted, showing exponential curves for soil temperature at depths of 5 and 10 cm from this equation:

$$F_{CO2} = \beta_0 \times e^{\beta 1 \times T}, \quad (2)$$

where $T$ is soil temperature (°C), and $\beta_0$ and $\beta_1$ are constants. This exponential relationship is commonly used to represent soil carbon efflux as a function of temperature (Davidson et al., 1998; Xu and Qi, 2001; Davidson and Janssens, 2006; Rayment and Jarvis, 2000; Kim et al., 2007, 2013). $Q_{10}$ temperature coefficient values were calculated as in Davidson et al. (1998) and Kim et al. (2013):

$$Q_{10} = e^{\beta 1 \times 10} \quad (3)$$

$Q_{10}$ is a measure of the change in reaction rate at intervals of 10 °C, based on Van't Hoff's empirical rule that a rate increase on the order of two to three times occurs for every 10 °C rise in temperature (Lloyd and Taylor, 1994).

## 2.3. Description of Hierarchical Bayesian (HB) model

To evaluate the relationship between $CO_2$ efflux and environmental variables, we modeled observed $CO_2$ efflux using an HB model with four explanatory variables: soil temperature (ST), soil moisture (SM), vegetation types (Vege), and thaw depth (THAW).

First, $CO_2$ efflux ($F_{CO2}$) was assumed normally distributed with mean parameter ($\mu_{flux}$) and variance parameter ($\sigma$):

$$F_{CO_2} \sim normal(\mu_{flux}, \sigma^2), \quad (4)$$

The scale parameter ($\mu_{flux}$) was determined from the following equation:

$$\mu_{flux} = f_P f_{ST} f_{SM} f_{THAW}, \quad (5)$$

where $f_P$ represents the function of $CO_2$ efflux potential, $f_T$ and $f_{SM}$ are limiting response functions, ranging from 0 to 1. $f_P$ was defined as follows:

$$f_P = \beta_0 + Vege_{[k]} + Year_{[l]} + Posi_{[ij]}, \quad (6)$$

in which $f_P$ is a linear predictor with intercept ($'\beta_0'$) and three random effects (*Vege*, *Year*, and *Posi*). The *Posi* term represents the spatial random effect of the conditional autoregressive model (CAR) proposed by Besag et al. (1991).

Temperature ($f_T$) uses a modified Van't Hoff equation as follows:

$$f_{ST} = e^{\frac{ST - ST_{ref}}{10} \log(Q_{10})}, \quad (7)$$

where $f_{ST}$ is the temperature response function, varying from 0 to 1. The explanatory variable of this function, represented by $ST$ and $ST_{ref}$, is a constant, set at 25 °C for this study. The temperature sensitivity parameter is shown by $Q_{10}$. The soil moisture limiting function ($f_{SM}$) is defined as follows:

$$f_{SM} = \left(\frac{SM-a}{b-a}\right)^a \left(\frac{SM-c}{b-c}\right)^{-d(b-c)/(b-a)}, \quad (8)$$

where the soil moisture response function, $f_{SM}$, ranges from 0 to 1, and is the same as the temperature response function (Hashimoto et al., 2010). *SM* is the explanatory variable of this function, and *a*, *b*, *c*, and *d* are the parameters for determining the shape of the soil moisture function. The function has a convex shape, and values range from 0 to 1. Parameters *a* and *c* are

1 the minimum and maximum values of SM, respectively (i.e., g(a) = g(c) = 0). Parameter *b*, which
2 ranges between *a* and *c*, is the optimum parameter (i.e., g(b) = 1). Parameter *d* controls the
3 curvature of the function, though the three other parameters also affect the shape. This function
4 was adopted from the DAYCENT model (Parton et al., 1996; Del Grosso et al., 2000).

5 $f_{THAW}$ is a function of thaw depth. We modeled this as follows:

6 $$f_{THAW} = \frac{1}{1 + e^{k - r\,THAW}}, \quad (9)$$

7 where the thaw depth function also ranges from 0 to 1. *THAW* is the explanatory variable of this
8 function, and *k* and *r* are the parameters. We assumed $CO_2$ efflux to monotonically increase
9 together with thaw depth (depth of active layer); however, these increases are not simply
10 proportional, due to carbon depth distribution.

11 Finally, we modeled the priors of each parameter. For vegetation, we incorporated a random
12 effect as follows:

13 $$Vege_k \sim normal(0, \sigma_{vege}); \quad (10)$$

14 $$Year_l \sim normal(0, \sigma_{year}). \quad (11)$$

15 For spatial explicit random effect, we used CAR modeling (Besag et al., 1991), as follows:

$$Posi_{il} \sim normal(b_{ij}, \frac{\sigma_{posi_{ij}}}{n})$$

16 $$b_{il} \sim \frac{1}{n_{ij}} \sum_{m=1}^{neighbors(ij)} b_m,$$

17 where $n_{ij}$ is the number of neighbors for neighborhood ij.

18 For priors, we defined as follows:

19 $\beta_0 \sim normal(0, 1000)$,
20 $Q_{10} \sim uniform(1, 10)$,

$$
\begin{aligned}
a &\sim uniform(-2, 0),\\
b &\sim uniform(0.1, 0.5),\\
c &\sim uniform(1, 3),\\
d &\sim uniform(0.01,\ 10),\\
k &\sim uniform(0, 10),\\
r &\sim uniform(0, 1),\\
\sigma^2 &\sim uniform(0,\ 100),\\
\sigma_{vege}^2 &\sim uniform(0, 100),\\
\sigma_{year}^2 &\sim uniform(0, 100),
\end{aligned}
\tag{12}
$$

For $\beta_0$, we used a normal distribution with mean 0 and a very large variance. Priors regarding soil moisture function (*a, b, c, d*) are based on Hashimoto et al. (2012). We set priors for $\sigma_{vege}^2$ and $\sigma_{year}^2$ to be vague, meaning large enough in value to accommodate the actual observed $CO_2$ efflux of this study.

The joint posterior probability was described as follows:

$$
\begin{aligned}
p(\theta|data) \propto \prod Normal(F_{CO_2}|\mu, \beta_{o,10}, a, b, c, d, k, r, \sigma_1, \sigma_{vege}, \sigma_{year}, \sigma_{posi}) \\
\times p(\beta_o) \times p(Q_{10}) \times p(a) \times p(b) \times p(c) \times p(d) \\
\times p(k) \times p(r) \times p(\sigma_1) \times p(\sigma_{vege}) \times p(\sigma_{year}) \times p(\sigma_{posi}),
\end{aligned}
\tag{13}
$$

where $p(\theta)$ denotes priors. For this model, we used MCMC methods implemented with Bayesian inference using the Gibbs sampling software WinBUGS (WinBUGS, version 1.4.3; D. Spiegelhalter et al., 2007, available at http://www.mrc-bsu.ac.uk/bugs), and the Gelman-Rubin convergence diagnostic as an index. For the model, we ran 20,000 Gibbs sampler iterations for three chains, with a thinning interval of 10 iternations. We discarded the first 10,000 iterations as burn-in, and used the remaining iterations to calculate posterior estimates. R was used to call JAGS/WinBUGS and calculate statistics in R.

## 3. Results and Discussion

### 3.1. $CO_2$ Efflux and Environmental Factors

Table 1 shows monthly average ± standard deviation (Coefficient of Variance, %) of $CO_2$ efflux, soil temperature at 5 and 10 cm below the surface, soil moisture, thaw depth, and pH in lichen, moss, tussock tundra, and grass during the growing seasons of 2011 and 2012. Annual growing season average $CO_2$ efflux is $4.6 \pm 2.5$ (54 %) and $3.1 \pm 2.0$ (66 %) $mgCO_2\,m^{-2}\,min^{-1}$ for 2011 and 2012, respectively. This indicates that growing season $CO_2$ efflux in 2011 was 1.5 times higher than in 2012, as well as the significance of heavy rainfall during the mid-growing season of 2012. $CO_2$ efflux in tussock tundra was approximately 1.8 times greater than in other plants, which may be due more to tussock's relatively wider surface area than others. While surface area in lichen and moss is 0.070 $m^2$—the same surface area of the measurement chamber—average surface area of tussock is $0.090 \pm 0.024$ $m^2$, based on an average height of $19.2 \pm 5.1$ cm. $CO_2$ efflux in the Arctic tundra of Alaska ranged from 0.38 to 1.6 $mgCO_2\,m^{-2}\,min^{-1}$ in lichen and 0.44 to 4.3 $mgCO_2\,m^{-2}\,min^{-1}$ in tussock during the growing season (Poole and Miller, 1982). Within tundra near Barrow, Alaska, meanwhile, $CO_2$ efflux in tussock and wet sedge was 0.23 and 0.022 $mgCO_2\ m^{-2}\ min^{-1}$, respectively (Oechel et al., 1997), suggesting that $CO_2$ efflux in tussock is indeed a more significant atmospheric $CO_2$ source than wet sedge. Kim et al. (2013) reported that tussock is an important source of carbon efflux to the atmosphere, contributing 3.4-fold more than other vegetation types in Alaska tundra and boreal forest systems. Further, tussock-originated $CO_2$ efflux, which occupies a circumpolar area ranging from $9 \times 10^{11}$ $m^2$ (Miller et al. 1983) to $6.5 \times 10^{12}$ $m^2$ (Whalen and Reeburgh, 1988) when counted with moss species, provides a quantitative understanding of a significant atmospheric carbon source from the Arctic terrestrial ecosystem. Considering the circumpolar distribution of tussock tundra and moss in the Arctic tundra ecosystem, $CO_2$ efflux measured in this study should not be overlooked in the evaluation of the regional/global carbon budget regarding distribution characteristics of on-ground plants.

The spatial distribution of $CO_2$ efflux within a 40 m × 40 m plot in 2011 and 2012 is shown in

Figure 2. $CO_2$ efflux in June 2011 was much higher than during other observation periods, reflecting the effects of higher air temperature and lower precipitation in June (see Figure 1). This further suggests an explicit difference in $CO_2$ efflux between June of 2011 and June 2012 within the plot, as shown in Table 1. We also note that $CO_2$ efflux in September 2012 rapidly decreased, due to heavy rainfall from mid-August to mid-September 2012. Within the plot, while the CV of monthly average $CO_2$ efflux in 2011 was prone to decrease, CV in 2012 tends to increase. This denotes a susceptibility to extreme environmental factors in 2012 compared to 2011.

Annual growing season average ± standard deviation for soil temperatures at 5 and 10 cm below the soil surface were 9.0 ± 4.2 (47 %) and 5.9 ± 3.9 °C (66 %) for 2011 and 7.7 ± 4.5 (58 %) and 5.7 ± 3.5 °C (61 %) for 2012, respectively. This indicates soil temperature in 2011 was higher than in 2012, similar to annual average $CO_2$ efflux, suggesting soil temperature is likely to modulate $CO_2$ efflux, as largely reported in regions worldwide (Davidson et al., 1998; Xu and Qi, 2001; Davidson and Janssens, 2006; Rayment and Jarvis, 2000; Kim et al., 2007; 2013). The spatial distribution of high/low soil temperature for each month was identical to the pattern of high/low $CO_2$ efflux, as also shown in Figure 2.

Annual average soil moisture was $0.253 \pm 0.158$ (CV: 62 %) $m^3 m^{-3}$ in 2011 and $0.272 \pm 0.180$ $m^3 m^{-3}$ (66 %) in 2012, indicating moisture in 2011 was slightly lower than in 2012. Soil moisture in September 2011 was not measured, due to damage to the soil moisture sensor. Spatial distribution of soil moisture is related to geographical topography, such as slope and relief within the plot, reflecting spatial distribution of lower $CO_2$ efflux and lower soil temperature in the trough area (not shown). Soil moisture, along with soil temperature, is also an important factor in the control of $CO_2$ efflux (Davidson et al., 1998; Gaumont-Guay et al., 2006; Mahecha et al., 2010; Kim et al., 2013).

Average thaw depth was 39 ± 5 (15 %) cm in 2011 and 38 ± 6 (15 %) cm in 2012, showing no significant difference, based on a one-way ANOVA at the 95 % confidence level ($p < 0.001$). The distribution of thaw depth (not shown) appears similar to the soil moisture pattern, which is inversely related to $CO_2$ efflux and soil temperature. The average thaw rate over our 81 points

was 0.43 cm $day^{-1}$ in 2011 and 0.41 cm $day^{-1}$ in 2012, reflecting that thaw rate over time remains almost constant during the growing season, and that thaw depth is not considered to regulate $CO_2$ efflux. In general, the deeper the active layer in response to permafrost thaw in the Arctic (Marchenko et al., 2008), the more $CO_2$ emission from the soil to the atmosphere (Elberling et al., 2013), also suggesting the potential decomposition of frozen, higher-stocked soil organic carbon (Ping et al., 2008; Tarnocai et al., 2009; Grosse et al., 2011). However, temporal variation in thaw depth of the active layer may not stimulate $CO_2$ production. This suggests the strength of $CO_2$ production that depends on soil microbial metabolism is affected more by environmental factors than constant active layer depth for both years. The deeper active layer reached to nearly 80 cm below the surface with the soil temperature profile at 50, 70, 80, and 92 cm from July 2012 to October 2013 (not shown). When the soil contained much higher soil moisture and much deeper thaw depth for September, pH represented a similar value of $3.8 \pm 0.4$ (11 %), representing an acidic tundra soil (pH < 5.5; Walker et al., 1998) among all points. The pH measurement was not conducted during the growing season of 2012, due to near uniformity within the plot.

### 3.2. Environmental Factors Determining $CO_2$ Efflux

$CO_2$ efflux is potentially modulated by environmental factors such as soil temperature, soil moisture, and thaw depth. $Q_{10}$ values were calculated using Eq. (3), based on the exponential relationship between $CO_2$ efflux and soil temperature at 5- and 10-cm depths for each plant. Table 2 shows $Q_{10}$ values and correlation coefficients between $CO_2$ efflux and soil temperature at 5- and 10-cm depths in lichen, moss, grass, and tussock tundra during the growing season, based on a one-way ANOVA with a 95 % confidence level. $Q_{10}$ is prone to increasing with time, suggesting that $CO_2$ production by soil microbes and roots has greater sensitivity to a narrower range of soil temperatures, such as in the spring and fall seasons (Rayment and Jarvis, 2000; Gaumont-Guay et al., 2006; Monson et al., 2006; Malcom et al., 2009). In this Alaska tundra ecosystem, average daily $CO_2$ efflux from wet sedge followed soil surface temperature closely, increasing exponentially as soil surface temperature increased, while efflux from the tussock tundra ecosystem followed soil surface temperature nearly logarithmically (Oechel et al., 1997).

In this study, the response from $CO_2$ efflux in tussock tundra to soil temperature depicts an almost linear relationship; however, it shows an exponential curve for $Q_{10}$ values, listed in Table 2. Soil temperature at 5-cm depth explained 86 % and 70 % of the variability in $CO_2$ efflux for 2011 and 2012, respectively, from the linear relationships, demonstrating that soil temperature is a significant factor in driving $CO_2$ efflux in dominated tundra plants during the growing season. The $Q_{10}$ value for soil temperature at 5-cm depth for the moss regime in August 2012 was the lowest, at 1.15, resulting from higher soil temperature and higher soil moisture in August 2012 (Table 1).

Figure 3 shows the responses from monthly averaged $CO_2$ efflux to soil temperature at 5- and 10-cm depths (a1 and b1), soil moisture (a2 and b2), and thaw depth (a3 and b3), and the responses from soil temperature at 5 cm to soil moisture (a4 and b4) and thaw depth (a5 and b5) during the growing seasons of 2011 and 2012. Except for a1 and b1, these relationships were each negatively related during the growing season of 2011-12. However, except for data measured in September 2012, these relationships denoted positive lines from June to August 2012, as also shown in Figure 3 (b2-5). This seems to be the effect of heavy rainfall beginning in August 20, 2012, as shown in Figure 1, which represents daily and cumulative precipitation in 2011 and 2012. Interestingly, cumulative rainfall indeed began to surpass 2011 cumulative precipitation on August 20, 2012 (not shown). The correlation coefficient ($R^2$) from June to August 2012 ranged from 0.01 in Figure 3 (b3) to 0.32 in (b2). Hence, soil moisture elucidated 32 % of the variability in $CO_2$ efflux before the severe rainfall event of the fall season of 2012, demonstrating that soil moisture is another important factor aside from soil temperature. Jensen et al. (2014) estimated $2.3 \pm 0.2$ and $1.3 \pm 0.11$ $mgCO_2\ m^{-2}\ min^{-1}$ in the northwestern tundra of Alaska in July of 2011 and 2012, respectively, suggesting lower carbon flux results from the stronger rainfall event in 2012 (see Figure 3a, Jensen et al., 2014), with a similar trend in air temperature between both years. This rainfall may have possibly inhibited 43 % of $CO_2$ emission from the soil surface with increasing soil moisture in 2012, indicating a similar result to those observed in this study (Davidson et al., 1998).

### 3.3. Simulated $CO_2$ Efflux from a Hierarchical Bayesian Model

We used 486 datasets of $CO_2$ efflux, soil temperature, soil moisture, vegetation types, and thaw depth for adjusting the parameters of a hierarchical Bayesian (HB) model, and the posterior distribution of the parameter for the $CO_2$ efflux is summarized in Table 3. Potential $CO_2$ effluxes from the dominated plants calculated from posterior medians of the model were 16.8 $mgCO_2\ m^{-2}\ min^{-1}$ in grass (95 % predicted credible intervals (CI), 13.7-20.4 $mgCO_2\ m^{-2}\ min^{-1}$), 15.3 $mgCO_2\ m^{-2}\ min^{-1}$ in lichen (95 % predicted CI, 11.1-16.8 $mgCO_2\ m^{-2}\ min^{-1}$), 14.8 $mgCO_2\ m^{-2}\ min^{-1}$ in moss (95 % predicted CI, 10.2-15.9 $mgCO_2\ m^{-2}\ min^{-1}$), and 21.9 $mgCO_2\ m^{-2}\ min^{-1}$ in tussock (95 % predicted CI, 24.0-31.0 $mgCO_2\ m^{-2}\ min^{-1}$). This suggests that the contribution of atmospheric carbon from tussock tundra should receive attention when it comes to the tundra ecosystem and a circumpolar scale response to the changing climate in the higher northern hemisphere (Oechel et al., 1997; Bhatt et al., 2010; 2013; Kim et al., 2013). We computed limiting functions for soil temperature, soil moisture, and thaw depth of $CO_2$ efflux simulated by posterior distributions (n = 1,000), as shown in Figure 4, for the quantitative assessment of the driving parameters for $CO_2$ efflux. Because changes in vegetation within the plot were not observed during this study period, these two parameters are not correlated with one another. In actuality, there was very low correlation ($R^2 = 0.019$) between $t_{veg}$ and $t_{year}$ in our results.

For soil temperature limiting functions, the parameter simulated from the posterior median followed soil temperature nearly exponentially (Figure 4a), demonstrating the definite temperature dependency of $CO_2$ efflux (Raich and Schlesinger, 1992; Davidson et al., 1998; Gaumont-Guay et al., 2006; Mahecha et al., 2010; Kim et al., 2013), as shown in Figure 3a1 and b1. For soil temperature response, the parameter $Q_{10}$ value was 2.52 ± 0.12 (95 % predicted CI, 2.29-2.75). For soil moisture limiting functions (Figure 4b), optimum soil moisture value was 0.228 $m^3\ m^{-3}$ (95 % predicted CI, 0.184-0.238 $m^3\ m^{-3}$). $CO_2$ efflux tended to increase with an increase in soil moisture when soil moisture value was at the optimum, as shown in Figure 3a2 and b2. On the other hand, the response from $CO_2$ efflux to soil moisture changed to a negative trend beyond the optimum value for soil moisture. The results from Jensen et al. (2014) proved

the findings observed in this study, in which $CO_2$ efflux was relatively lower with the higher soil moisture observed in 2012, compared to 2011 (see Figure 4b, Jensen et al., 2014). Davidson et al. (1998) reported the correlation between soil water content and $CO_2$ efflux in different drainage classes. $CO_2$ efflux increased when soil water content was less than 0.2 $m^3$ $m^{-3}$; on the other hand, higher soil moisture resulted in a decrease in $CO_2$ efflux (see Figure 7, Davidson et al., 1998). For thaw depth limiting functions, the parameter increased to 20 cm, which represents the optimum thaw depth value (Figure 4c). While $CO_2$ efflux increased with the rise in thaw depth in June until optimum thaw depth value, efflux was constant, despite an increase in thaw depth with time. The response from $CO_2$ efflux to thaw depth turned to a negative trend during the growing seasons of 2011 and 2012, as shown in Figure 3a3 and b3. These findings suggest that thaw depth may not be a significant parameter in influencing $CO_2$ efflux in the tundra ecosystem, in spite of a deeper active layer over time.

Spatial distribution of simulated $CO_2$ efflux, calculated from the posterior medians of the hierarchical Bayesian model during the growing seasons of 2011 and 2012 and excluding July and September of 2011, is similar to that of measured $CO_2$ efflux, as shown in Figure 2. The pattern of simulated $CO_2$ efflux is nearly identical to the spatial distribution of measured $CO_2$ efflux (Figure 3), as simulated $CO_2$ efflux is a function of soil temperature, soil moisture, and thaw depth. Of these, we consider soil temperature the most important parameter in modulating $CO_2$ efflux in the tundra ecosystem during the growing season. We compared measured $CO_2$ efflux to predicted $CO_2$ efflux using posterior medians in the HB model at each sampling period of 2011 and 2012 (Figure 5), denoting that $CO_2$ efflux simulated by a nonlinear equation is consistent with measured data. Using the HB model, cumulative predicted $CO_2$ emission rates from June 28 to September 30 of 2011 and 2012—based on monitored soil temperature and soil moisture in the Council area—were 742 $gCO_2$ $m^{-2}$ $period^{-1}$ (95 % predicted CI, 646-839 $gCO_2$ $m^{-2}$ $period^{-1}$) and 539 $gCO_2$ $m^{-2}$ $period^{-1}$ (95 % predicted CI, 460-613 $gCO_2$ $m^{-2}$ $period^{-1}$), respectively. These findings suggest that the 2012 $CO_2$ emission rate is constrained by 27 % (95 % CI, 17-36 %) compared to the 2011 emission, demonstrating that higher soil moisture from severe rain constrains the emission of soil-produced $CO_2$ to the atmosphere (Jensen et al., 2014).

During the study periods (DOY: 179-273; Figure 6) of 2011 and 2012, average soil temperature was 9.3 ± 3.8 (CV: 41 %) and 8.6 ± 4.8 (CV: 56 %) °C, respectively, showing that there is no significant difference between the years, based on a one-way ANOVA 95 % confidence level. Trends in soil temperature during the periods of 2011 and 2012 were ST = -0.135 × DOY + 5522 ($R^2$ = 0.70), and ST = -0.093 × DOY + 3781 ($R^2$ = 0.45), respectively. On the other hand, trends for soil moisture were SM = 0.0025 × DOY - 103.5 ($R^2$ = 0.37) in 2011 and SM = -0.0008 × DOY + 33.2 ($R^2$ = 0.31) in 2012, as shown in 6. Average soil moisture was 0.260 ± 0.040 (15 %) and 0.493 ± 0.124 (25 %) $m^3 m^{-3}$ in 2011 and 2012, respectively, suggesting a distinct difference in soil moisture between the two years. Soil moisture during the 2012 period did not change with time, resulting from heavy rainfall events (Figure 1) during the growing season (Jensen et al., 2014). When soil temperature at the end of September in 2012 was below zero (Figure 6a), soil moisture sharply decreased, suggesting the frozen layer reached to soil moisture measuring depth (e.g., near surface), as shown in Figure 6b. The 2012 weather conditions may represent an episodic event, requiring additional monitoring for several representative points within the plot. Nevertheless, the higher $CO_2$ emission rate simulated by the HB model in 2011 is considered likely the result of $CO_2$ efflux increases until soil moisture reached optimum value, as shown in Figures 4b. Therefore, soil moisture plays an important parameter in constraining $CO_2$ emission in this tundra ecosystem, when the soil moisture is over the optimum value. When the annual simulated $CO_2$ emission rate was estimated from the relationship between $CO_2$ efflux and air temperature using equation (2), the annual emission rates were 827 and 609 $gCO_2 m^{-2} year^{-1}$ in 2011 and 2012, respectively, corresponding to 86 and 80 % of annual $CO_2$ emission rates. Kim et al. (2013) estimated growing season $CO_2$ emission in the foothill tundra north of Brooks Range, Alaska was 645 $gCO_2 m^{-2} period^{-1}$ during 2006-2010, despite the difference in latitudinal distributions for $CO_2$ efflux and parameter. This value is situated between the 2011 and 2012 emission rates simulated in Council in this study. That is, the simulated $CO_2$ emission rates were 0.86-1.20 $MgCO_2$ within a 40 m × 40 m plot during the growing seasons of 2012 and 2011, respectively.

## 4. Summary and Future Works

Here, $CO_2$ efflux measurement was conducted with a manual chamber system in the tundra ecosystem of the Seward Peninsula of western Alaska, during the growing seasons of 2011 and 2012, to evaluate the significant parameter(s) controlling $CO_2$ efflux, as well as the effect(s) on the soil-produced $CO_2$ emission rate to the atmosphere, using a hierarchical Bayesian (HB) model within a 40 m × 40 m plot (5-m interval; 81 points). Tussock tundra is an atmospheric carbon source in the tundra ecosystem year-round (Oechel et al., 1997; Kim et al., 2007, 2013). Considering the wide-ranged distribution of tussock in the high Northern Hemisphere, tussock- and moss-originated $CO_2$ efflux should not be overlooked as a significant carbon source in the estimation of regional and global carbon budgets. The response from $CO_2$ efflux in tussock to soil temperature denoted a linear relationship; meanwhile, effluxes observed in lichen and moss regimes increased exponentially as soil temperature increased. This finding suggests that soil temperature is a key environmental factor in modulating $CO_2$ efflux, as many scientists have also reported around the world. Except for data observed in September 2012, soil moisture played an important factor in controlling $CO_2$ efflux. For 2012, higher soil moisture, resulting from the heavy rainfall in the end of August, was a constraining factor for the transport of soil-produced carbon to the atmosphere (Davidson et a l., 1998; Jensen et al., 2014).

Using the HB model, we computed limiting functions for soil temperature, soil moisture, and thaw depth of $CO_2$ efflux simulated by posterior distribution. Simulated $CO_2$ efflux increased both 1) exponentially as soil temperature increased and 2) nearly linearly until soil moisture was at optimum values (0.228 $m^3$ $m^{-3}$); however, efflux decreased 3) logarithmically when soil moisture was beyond the optimum, and 4) nearly linearly until thaw depth was at optimum value (20 cm). Finally, efflux remained constant when thaw depth increased with time. These simulated findings show similar patterns to the data obtained in this study, as well as to Jensen et al. (2014)'s results observed in the northwestern tundra of Alaska during the growing seasons of 2011 and 2012. During these growing seasons of 2011 and 2012, the difference in soil temperature between the two years was not significant; however, there was a distinct difference in soil moisture between them, resulting in the inhibition of $CO_2$ emissions due to higher soil

moisture. This demonstrates that higher soil moisture is constrained to 27 % of the $CO_2$ emission in 2012 compared to 2011. However, to prove the effect of soil moisture on controlling $CO_2$ emission in the tundra ecosystem, additional study must monitor the profiles of soil moisture and soil temperature at representative points from lichen, moss, and tussock tundra regimes within the plot. As conducted by Risk et al. (2011), the monitoring of soil $CO_2$ efflux must also show representative points, along with the monitoring of environmental factor profiles within the plot.

## Acknowledgments

This work was supported by the National Research Foundation of Korea Grant funded by the Korean Government (MSIP) (NRF-C1ABA001-2011-0021063) (Title: Establishment of Circum-Arctic Permafrost Environment Change Monitoring Network and Future Prediction Techniques (CAPEC Project)). This research was conducted under the JAMSTEC-IARC Collaboration Study, with funding provided by the Japan Agency for Marine-Earth Science and Technology (JAMSTEC), as well as the IARC-JAXA Information System (IJIS), with funding partly provided by the Japan Aerospace Exploration Agency (JAXA) under a grant to the International Arctic Research Center (IARC).

## References


ACIA (Arctic Climate Impact Assessment): Impacts of a Warming Arctic, Cambridge Univ. Press, Cambridge, U.K., 146 pp, 2004.

Besag, J., York, J.C., Molife, A.: Bayesian image restoration with two applications in spatial statistics, Ann. Inst. Stat. Math., 43, 1-59, 1991.

Bhatt, U. S., Walker, D. A., Raynolds, M. K., Comiso, J. C., Epstein, H. E., Jia, G., Gens, R., Pinzon, J. E., Tucker, C. J., Tweedie, C. E., Webber, P. J.: Circumpolar arctic tundra vegetation change is linked to sea ice decline, Earth Interactions, 14, 1–20, DOI: 10.1175/2010EI315.1, 2010.

Bhatt, U. S., Walker, D. A., Raynolds, M. K., Bieniek, P. A., Epstein, H. E., Comis, J. C., Pinzon, J. E., Tucker, C. J., and Polyako, I. V.: Recent declines in warming and vegetation greening trends over pan-Arctic tundra, Remote Sens., 5, 4229-4254, doi:10.3390/rs5094229, 2013.

Bond-Lamberty, B., Thomson, A.: Temperature-associated increases in the global soil respiration record, Nature, 464, 597–582, 2010.

Clark, J. S.: Why environmental scientists are becoming Bayesians, Ecol. Lett., 8(1), 2-14, doi:10.1111/j.1461-0248.2004.00702.x, 2005.

Davidson, E. A., Belk, E., Boone, R. D.: Soil water content and temperature as independent or confounded factors controlling soil respiration in a temperate mixed hardwood forest, Global Change Biol., 4, 217–227, 1998.

Davidson, E. A., Savage, K., Verchot, L. V., and Bavarri, R.: Minimizing artifacts and biases in chamber-based measurements of soil respiration, Argicul. Forest Meteol., 113:21-37, 2002.

Davidson, E. A., Janssens, I. A.: Temperature sensitivity of soil carbon decomposition and feedback to climate change, Nature, 440, 165–173, 2006.

Del Grosso, S. J., Parton, W. J., Mosier, A. R., Ojima, D. S., Potter, C. S., Borken, W.,Brumme, R., Butterbach-Bahl, K., Crill, P. M., Dobbie, K., Smith, K. A.: General $CH_4$ oxidation model and comparisons of $CH_4$ oxidation in natural and managed systems, Global Biogeochem. Cycles, 14, 999–1019, 2000.

Elberling, B., and Brandt, K. K.: Uncoupling of microbial $CO_2$ production and release in frozen soil and its implications for field studies of arctic C cycling, Soil Biol. Biochem., 35(2), 263-272, 2003.

Elberling, B., Michelsen, A., Schädel, C., Schuur, E. A. G., Christiansen, H. H., Berg, L., Tamstorf, M., and Sigsgaard, C.: Long-term $CO_2$ production flowing permafrost thaw, Nature Climate Change, 3, 890-894, doi:10.1038/nclimate1955, 2013.

Gaumont-Guay, D., Black, T. A., Griffis, T. J., Barr, A. G., Jassal, R. A., and Nesic, Z.: Interpreting the dependence of soil respiration on soil temperature and water content in a boreal aspen stand, Agr. Forest Meteorol., 140:220-235, 2006.

Grosse, G., Harden, J., Turetsky, M., McGuire, A. D., Camill, P., Tarnocai, C., Frolking, S., Schuur, E. A. G., Jorgenson, T., Marchenko, S., Romanovsky, V., Wickland, K. P., French, N., Waldrop, M., Bourgeau-Chaves, L., and Striegl, R. G.: Vulnerability of high-latitude soil organic carbon in North America to disturbance, J. Geophys. Res., 116, G00K06, doi:10.1029/2010JG001507, 2011.

Hashimoto, S., Morishita, T., Sakata, T., Ishizuka, S., Kaneko, S., and Takahashi, M.: Simple models for soil $CO_2$, $CH_4$, and $N_2O$ fluxes calibrated using a Bayesian approach and multi-site data, Ecol. Modelling, 222, 1283-1292, 2011.

Hinzman, L. D., Bettez, N. D., Bolton, W. R., Chapin, F. S., Dyurgerov, M. B., Fastie, C. L., Griffith, B., Hollister, R. D., Hope, A., Huntington, H. P., Jensen, A. M., Jia, G. J., Jorgenson, T., Kane, D. L., Klein, D. R., Kofinas, G., Lynch, A. H., Lloyd, A. H., McGuire, A. D., Nelson, F. E., Oechel, W. C., Osterkamp, T. E., Racine, C. H., Romanovsky, V. E., Stone, R. S., Stow, D. A., Sturm, M., Tweedie, C. E., Vourlitis, G. L., Walker, M. D., Walker, D. A.,

Webber, P. J., Welker, J. M., Winker, K. S., and Yoshikawa, K.: Evidence and implications of recent climate change in northern Alaska and other arctic regions, Climatic Change 72:251-298, 2005.

Hutchinson, G. L., and Livingston, P.: Soil-atmosphere gas exchange. In: Dane, J. H., Topp, G. C. (eds) Mehtods of soil analysis: Part 4, Physical methods, 3rd edn. Book Series 5. Madison, WI, Soil Science Society of America, pp 1159-1182, 2002.

Jensen, A. E., Lohse, K. A., Crosby, B. T., Mora, C. I.: Variations in soil carbon dioxide efflux across a thaw slump chronosequence in northwestern Alaska, Environ. Res. Lett. 9, 025001, 2014.

Kim, Y., Ueyama, M., Nakagawa, F., Tsunogai, U., Tanaka, N., Harazono, Y.: Assessment of winter fluxes of $CO_2$ and $CH_4$ in boreal forest soils of central Alaska estimated by the profile method and the chamber method: A diagnosis of methane emission and implications for the regional carbon budget, Tellus 59B, 223–233, 2007.

Kim, Y., Kim, S. D., Enomoto, H., Kushida, K., Kondoh, M., and Uchida, M.: Latitudinal distribution of soil $CO_2$ efflux and temperature along the Dalton Highway, Alaska. Polar Sci., 7, 162-173, 2013.

Koven, C. D., Ringeval, B., Friedlingstein, P., Ciais, P., Cadule, P., Khvorostyanov, D., Krinner, G., and Tarnocai, C.: Permafrost carbon-climate feedbacks accelerate global warming, Proc. Nat. Acad. Sci. USA, 108:14769-14774, 2011.

Lloyd, J., Taylor, J. A.: On the temperature dependence of soil respiration. Functional Ecol. 8, 315–323, 1994.

Mahecha, M. D., Reichstein, M., Carvalhais, N., Lasslop, G., Lange, H., Seneviratne, S. I., Vargas, R., Ammann, C., Arain, M. A., Cescatti, A., Janssens, I. A., Migliavacca, M., Montagnani, L., and Richardson, A. D.: Global convergence in the temperature sensitivity of respiration at ecosystem level, Science, 329, 838-840, DOI: 10.1126/science.1189587, 2010.

Malcom, G. M., López-Gutiérres, J., and Koide, R. T.: Temperature sensitivity of respiration differs among forest floor layers in a *Pinus resinosa* plantation, Soil Biol. Biochem., 41:1075-1079, 2009.

Marchenko, S., Romanovsky, V., and Tipenko, G.: Numerical modeling of spatial permafrost dynamics in Alaska, in Proceedings of the Ninth International Conference on Permafrost, edited by Kane, D. L., and Hinkel, K. M., Inst. of North. Eng., Univ. of Alaska Fairbanks, Fairbanks, 1125–1130, 2008.

Michaelson, G. J., and Ping, C. L.: Soil organic carbon and $CO_2$ respiration at subzero temperature in soils of Arctic Alaska, J. Geophys. Res., 108, 8164, doi:10.1029/2001JD000920, 2003.

Miller, P. C., Kendall, R. and Oechel, W. C.: Simulating carbon accumulation in northern ecosystems, Simulation, 40:119-131, 1983.

Monson, R. K., Lipson, D. L., Burns, S. P., Turnipseed, A. A., Delany, A. C., Williams, M. W., and Schmidt, S. K.: Winter forest soil respiration controlled by climate and microbial community composition, Nature, 439, doi:10.1038/nature04555, 2006.

Nishina, K., Takenaka, C., Ishizuka, S.: Spatial variations in nitrous oxide and nitric oxide emission potential on a slope of Japanese ceder (*Cryptomeria japonica*) forest, Biogeochemistry, 96(1), 163-175, 2009.

Nishina, K., Akiyama, H. Nishimura, S., Sudo, S., and Yagi, K.: Evaluation of uncertainties in $N_2O$ and NO fluxes from agricultural soil using a hierarchical Bayesian model, J. Geophys. Res., 117, G04008, doi:10.1029/2012JG002157, 2012.

Oberbauer, S. F., Gillespie, C. T., Cheng, W., Gebauer, R., Sala Serra, A., Tenhunen, J. D.: Environmental effects on $CO_2$ efflux from riparian tundra in the northern foothills of the Brooks Range, Alaska, USA, Oecol., 92:568-577, 1992.

1 Oberbauer, S. F., Tweedie, C. E., Welker. J. M., Fahnestock, J. T., Henry, G. H. R., Webber, P. J.,
2 Hillister, R. D., Waler, M. D., Kuchy, A., Elmore, E., and Starr, G.: Tundra $CO_2$ fluxes in
3 response to experimental warming across latitudinal and moisture gradients, Ecol. Monogr.,
4 72:221-238, 2007.

5 Oechel, W. C., Vourlitis, G., Hastings, S. J.: Cold season $CO_2$ emissions from arctic soils, Global
6 Biogeochem. Cycles 11, 163–172, 1997.

7 Oechel, W. C., Vourlitis, G., Hastings, S. J., Zulueta, R. C., Hinzman, L. D., and Kane, D.:
8 Acclimation of ecosystem $CO_2$ exchange in the Alaska Arctic in response to decadal climate
9 warming, Nature, 406:978-981, 2000.

10 Parton, W.J., Mosier, A.R., Ojima, D.S., Valentine, D.W., Schimel, D.S., Weier, K., Kulmala,
11 A.E.: Generalized model for $N_2$ and $N_2O$ production from nitrification and denitrification,
12 Global Biogeochem. Cycles, 10, 401–412, 1996.

13 Ping, C. L., Michaelson, G. J., Jorgenson, M. T., Kimble, J. H., Epstein, H., Romanovsky, V.,
14 and Walker, D. A.: High stock of soil organic carbon in the North American Arctic region,
15 Nature Geosci., 1, 615-619, doi:10.1038/ngeo284, 2008.

16 Poole, K. D., and Miller, P. C.: Carbon dioxide flux from three Arctic tundra types in
17 North-Central Alaska, U.S.A., Arctic Alp. Res., 14, 27-32, 1982.

18 Post, E., Bhatt, U. S., Bitz, C. M., Brodie, J., Fulton, T. L., Hebblewhite, M., Kerby, J., Kutz, S.,
19 Stirling, J. K., and Walker, D. A.: Ecological consequences of Sea-ice decline, Science 341,
20 519, doi: 10.1126/science.1235225, 2013.

21 R Development Core Team: *R: A Language and Environment for Statistical Computing*, R Found.
22 Comput. Vienna (Available at http://www. R-project.org/), 2012.

23 Raich, J. W., and Schlesinger, W. H.: The global carbon dioxide flux in soil respiration and its
24 relationship to vegetation and climate, Tellus, 44B, 81–99, 1992.

Rayment, M. B., Jarvis, P. G.: Temporal and spatial variation of soil $CO_2$ efflux in a Canadian boreal forest. Soil Biol. Biochem., 32, 35–45, 2000.

Risk, D., Nickerson, N., Creelman, C., McArthur, G., Owens, J.: Forced diffusion soil flux: A new technique for continuous monitoring of soil gas efflux, Agr. For. Meteorol. 151, 1622–1631, 2011.

Romanovsky, V., Burgess, M., Smith, S., Yoshikawa, K., and Brown, J.: Permafrost temperature records: indicators of climate change, EOS transaction 80:589-594, 2002.

Savage, K. E., Davidson, E. A.: A comparison of manual and automated systems for soil $CO_2$ flux measurements: trade-offs between spatial and temporal resolution, J. Exper. Botany, 54, 891–899, 2003.

Schlesinger, W. H., and Andrews, J. A.: Soil respiration and the global carbon cycle, Biogeochemistry, 48, 7–20, 2000.

Schuur, E. A. G., Vogel, J. G., Crummer, K. G., Lee, H., Sickman, J. O., and Osterkamp, T. E.: The effect of permafrost thaw on old carbon release and net carbon exchange from tundra, Nature, 459, 556-559, doi:10.1038/nature0803, 2009.

Smith, L. C., Sheng, Y., MacDonal, G. M., and Hinzman, L. D.: Disappearing Arctic lakes, Science, 308:1427, 2005.

Spiegelhalter, D. T. A., and Best, N.: WinBUGS user manual, MRC Biostatistics Unit, Cambridge, UK, 2000.

Sturm, M., J. Schimel, J., Michaelson, G., Welker, J. M., Oberbauer, S. F., Liston, G. E., Fahnestock, J., and Romanovsky, V.: Winter biological processes could help convert Arctic tundra to shrubland, Biosci., 55, 17-26, 2005.

Tarnocai, C., Canadell, J. G., Schuur, E. A. G., Kuhry, P., Mazhitova, G., and Zimov, S.: Soil organic carbon pools in the northern circumpolar permafrost region, Global Biogeochem. Cycles, 23, GB2023, doi:10.1029/2008GB003327, 2009.

Walker, D. A., Auerbach, N. A., Bockheim, J. G., Chapin III, F. S., Eugster, W., King, J. Y., McFadden, J. P., Michaelson, G. J., Nelson, F. E., Oechel, W. C., Ping, C. L., Reeburg, W. S., Regli, S., Shiklomanov, N. I., Vourlitis, G. L.: Energy and trac-gas fluxes across a soil pH boundary in the Arctic, Nature, 394, 469-472, 1998.

Walter, K. M., Smith, L. C., and Chapin, F. S.: Methane bubbling from northern lakes: present and future contributions to the global methane budget, Phil. Trans. R. Soc. A., 365:1657-1676, 2007.

Whalen, S. C., Reeburgh, W. S.: A methane flux time series for tundra environments, Global Biogeochem. Cycles 5, 261–273, 1988.

Xu, M., and Qi, Y.: Soil-surface $CO_2$ efflux and its spatial and temporal variations in a young ponderosa pine plantation in northern California, Global Change Biol., 7, 667–677, 2001.

Yoshikawa, K., and Hinzman, L. D.: Shrinking thermokarst ponds and groundwater dynamics in discontinuous permafrost near Council, Alaska, Permafrost Periglac. Processes, 14:151-160, 2003.

## Figure Legends

Figure 1. Average daily ambient temperature and precipitation in Council, Seward Peninsula, Alaska during April-October of 2011 and 2012 (Western Regional Climate Center). Dotted arrows denote that cumulative rainfall in 2012 exceeds that of 2011, beginning August 20, 2012.

Figure 2. Spatial distribution of $CO_2$ efflux ($mgCO_2\ m^{-2}\ min^{-1}$) within a 40 m × 40 m plot (5-m interval; 81 points), Council, Seward Peninsula, Alaska during the growing seasons of 2011 (upper panel) and 2012 (lower). Due to heavy rain in early July 2011, this data could not be measured, as shown in Figure 1.

Figure 3. Responses from monthly average $CO_2$ efflux to (1) average soil temperature at 5 and 10 cm (open and solid circles), (2) average soil moisture, and (3) thaw depth, as well as responses from average soil temperature at 5 cm to (4) average soil moisture and (5) average thaw depth during the growing seasons of (a) 2011 and (b) 2012. Dashed curves (a1 and b1) and dotted lines indicate the relationship between the two. Furthermore, solid lines in b2-5 denote the relationship between factors, except for data measured in September.

Figure 4. Limiting functions for (a) soil temperature, (b) soil moisture, and (c) thaw depth of $CO_2$ efflux simulated by posteriors (n = 1000). Red solid lines are simulated from posterior median.

Figure 5. Response from measured $CO_2$ efflux on simulated $CO_2$ efflux by posterior medians in the HB model as a function of soil temperature, soil moisture, and thaw depth within a 40 m × 40 m plot (5-m interval; 81 points), Council, Seward Peninsula, Alaska during the growing seasons of 2011 and 2012. (Reviewer #2)

Figure 6. Temporal variations in (a) soil temperature (°C) and (b) soil moisture ($m^3\ m^{-3}$), measured for tundra sites during the growing seasons of 2011 (black) and 2012 (red). When soil temperature was below zero, at the end of September 2012, soil moisture dropped rapidly, as shown in Figure 1.

*Supplementary material: Convergence plot of all HB model parameters

Table 1. Average ± standard deviation (coefficient of variation, %) of $CO_2$ efflux, soil temperature at 5 and 10 cm below the surface, soil moisture, thaw depth, and pH in lichen, moss, and tussock tundra, Council, Seward Peninsula, Alaska during growing seasons of 2011 and 2012

| Month | Vegetation | n | $CO_2$ efflux ($mgCO_2/m^2/min$) | Soil temperature (°C) 5 cm | Soil temperature (°C) 10 cm | Soil moisture ($m^3/m^3$) | Thaw depth (cm) | pH |
|---|---|---|---|---|---|---|---|---|
| June, 2011 | Lichen | 22 | 5.7±3.6 (63) | 10.1±2.5 (25) | 3.3±1.4 (42) | 0.270±0.162 (60) | 22±3 (12) | n.m.[#] |
| | Moss | 43 | 7.8±2.2 (29) | 13.2±2.9 (22) | 6.7±2.8 (42) | 0.224±0.122 (54) | 21±3 (14) | n.m. |
| | Tussock | 16 | 12.9±6.2 (48) | 12.7±3.3 (26) | 7.6±3.7 (48) | 0.301±0.116 (39) | 22±2 (11) | n.m. |
| | Average | 81* | 8.0±3.6 (45) | 12.3±3.2 (53) | 6.0±3.1 (51) | 0.255±0.127 (49) | 21±3 (14) | |
| August, 2011 | Lichen | 24 | 2.5±1.2 (47) | 6.9±1.5 (22) | 4.4±1.1 (25) | 0.297±0.200 (67) | 38±5 (14) | n.m. |
| | Moss | 41 | 3.3±1.7 (52) | 9.0±1.6 (18) | 6.2±1.7 (27) | 0.264±0.237 (90) | 41±8 (19) | n.m. |
| | Tussock | 16 | 5.1±2.7 (53) | 9.4±2.4 (25) | 7.0±2.1 (30) | 0.256±0.141 (55) | 40±5 (12) | n.m. |
| | Average | 81* | 3.3±1.3 (39) | 8.6±1.9 (22) | 5.8±1.4 (24) | 0.272±0.180 (66) | 40±6 (15) | |
| September, 2011 | Lichen | 23 | 2.3±0.9 (40) | 6.2±1.0 (16) | 4.6±1.0 (21) | -[**] | 57± 8 (13) | 3.7±0.4 (7) |
| | Moss | 43 | 2.5±1.2 (50) | 6.9±1.4 (20) | 5.6±1.3 (23) | - | 58±12 (20) | 3.8±0.4 (11) |
| | Tussock | 15 | 3.5±1.5 (43) | 6.5±1.4 (22) | 5.2±1.3 (25) | - | 55± 5 (8) | 3.8±0.3 (8) |
| | Average | 81* | 2.6±0.8 (30) | 6.0±1.6 (26) | 5.3±1.1 (21) | - | 57± 9 (16) | 3.8±0.4 (11) |
| June, 2012 | Lichen | 25 | 3.7±2.0 (53) | 11.1±3.0 (27) | 5.9±2.6 (44) | 0.213±0.113 (53) | 22±3 (12) | -[**] |
| | Moss | 38 | 4.7±1.8 (39) | 12.7±2.4 (19) | 7.1±2.3 (32) | 0.189±0.097 (51) | 21±3 (16) | - |
| | Tussock | 14 | 5.6±1.9 (33) | 12.2±2.4 (19) | 8.8±2.5 (29) | 0.339±0.136 (40) | 21±2 (11) | - |
| | Grass | 4 | 5.2±2.1 (40) | 10.4±3.0 (28) | 6.4±2.1 (33) | 0.304±0.149 (49) | 21±2 (8) | - |
| | Average | 81* | 4.8±2.0 (42) | 11.5±2.6 (23) | 6.6±2.5 (38) | 0.224±0.125 (56) | 21±3 (14) | |
| July, 2012 | Lichen | 25 | 4.0±1.5 (38) | 10.1±2.1 (21) | 6.9±1.8 (26) | 0.165±0.088 (53) | 33±3 (9) | -[**] |
| | Moss | 38 | 4.3±1.5 (35) | 11.2±2.4 (22) | 7.9±1.9 (25) | 0.243±0.086 (60) | 31±4 (13) | - |
| | Tussock | 14 | 5.9±2.8 (48) | 10.5±2.5 (23) | 7.9±2.5 (31) | 0.268±0.140 (52) | 31±2 (8) | - |
| | Grass | 4 | 5.6±1.9 (34) | 9.9±1.1 (11) | 6.6±1.0 (15) | 0.208±0.088 (42) | 36±6 (16) | - |
| | Average | 81* | 5.0±2.0 (40) | 11.3±2.2 (19) | 7.2±2.4 (33) | 0.191±0.118 (62) | 33±6 (18) | |
| August, 2012 | Lichen | 25 | 3.3±1.1 (33) | 13.0±2.6 (20) | 9.3±2.2 (23) | 0.201±0.117 (58) | 45±4 (10) | -[**] |
| | Moss | 38 | 4.7±1.6 (35) | 16.0±2.5 (15) | 11.9±2.7 (22) | 0.258±0.115 (73) | 44±7 (15) | - |
| | Tussock | 14 | 6.4±2.1 (33) | 16.2±2.5 (15) | 12.6±4.0 (32) | 0.288±0.120 (42) | 43±3 (7) | - |
| | Grass | 4 | 5.5±2.4 (43) | 13.2±0.8 (6) | 9.3±1.2 (13) | 0.199±0.069 (35) | 47±11 (22) | - |
| | Average | 81* | 4.8±1.9 (40) | 15.0±2.9 (19) | 11.0±3.2 (29) | 0.246±0.126 (51) | 45±6 (13) | |
| September, 2012 | Lichen | 25 | 1.6±0.9 (54) | 3.5±1.9 (55) | 2.1±1.6 (75) | 0.465±0.260 (56) | 59±7 (11) | -[**] |
| | Moss | 38 | 1.8±0.8 (44) | 4.9±2.3 (47) | 3.1±1.8 (59) | 0.340±0.264 (78) | 60±9 (16) | - |
| | Tussock | 14 | 2.3±1.0 (44) | 5.9±2.5 (42) | 4.1±2.0 (48) | 0.427±0.121 (28) | 57±4 (7) | - |
| | Grass | 4 | 2.2±0.9 (40) | 2.9±2.5 (26) | 2.0±1.6 (82) | 0.456±0.378 (82) | 64±9 (14) | - |
| | Average | 81* | 1.9±0.8 (42) | 4.4±2.2 (50) | 2.7±1.8 (65) | 0.424±0.262 (62) | 60±8 (13) | |

* denotes total measured points.

** - is not conducted.

[#] n.m. indicates not measured.

Table 2. $Q_{10}$ values and correlation coefficient between $CO_2$ efflux and soil temperature at 5 and 10 cm below the soil surface in lichen, moss, and tussock during the growing season based on a one-way ANOVA with a 95% confidence level

| Vegetation, Year | Month | 5 cm | | | 10 cm | | |
|---|---|---|---|---|---|---|---|
| | | $Q_{10}$ | $R^2$ | *p* | $Q_{10}$ | $R^2$ | *p* |
| Lichen, 2011 | June | 2.05 | 0.10 | <0.001 | 1.68 | 0.01 | 0.018 |
| | August | 8.58 | 0.36 | <0.001 | 2.47 | 0.04 | <0.001 |
| | September | 10.59 | 0.43 | <0.001 | 6.87 | 0.32 | <0.001 |
| | Total | 4.97 | 0.34 | <0.001 | 1.06 | 0.01 | 0.032 |
| Moss, 2011 | June | 1.58 | 0.26 | <0.001 | 1.54 | 0.15 | 0.073 |
| | August | 6.59 | 0.40 | <0.001 | 5.88 | 0.41 | <0.001 |
| | September | 7.54 | 0.28 | <0.001 | 10.10 | 0.78 | <0.001 |
| | Total | 5.05 | 0.62 | <0.002 | 4.46 | 0.21 | <0.001 |
| Tussock, 2011 | June | 2.68 | 0.54 | 0.890 | 2.01 | 0.33 | 0.005 |
| | August | 8.66 | 0.68 | <0.001 | 11.70 | 0.66 | 0.041 |
| | September | 10.74 | 0.58 | <0.001 | 9.64 | 0.44 | 0.008 |
| | Total | 6.15 | 0.73 | 0.018 | 5.44 | 0.39 | 0.467 |
| Lichen, 2012 | June | 4.03 | 0.66 | <0.001 | 1.40 | 0.24 | <0.001 |
| | July | 5.04 | 0.69 | <0.001 | 0.57 | 0.65 | <0.001 |
| | August | 2.41 | 0.46 | <0.001 | 2.50 | 0.35 | <0.001 |
| | September | 6.17 | 0.57 | <0.001 | 9.55 | 0.59 | <0.001 |
| | Total | 2.86 | 0.65 | <0.001 | 1.09 | 0.19 | <0.001 |
| Moss, 2012 | June | 2.62 | 0.37 | <0.001 | 0.95 | 0.01 | <0.001 |
| | July | 3.82 | 0.66 | <0.001 | 3.51 | 0.51 | <0.001 |
| | August | 1.15 | 0.01 | <0.001 | 1.14 | 0.01 | <0.001 |
| | September | 2.10 | 0.16 | <0.001 | 2.18 | 0.11 | <0.001 |
| | Total | 2.44 | 0.54 | <0.001 | 2.35 | 0.33 | <0.001 |
| Tussock, 2012 | June | 5.06 | 0.77 | <0.001 | 4.59 | 0.68 | <0.001 |
| | July | 3.78 | 0.73 | <0.001 | 2.78 | 0.50 | <0.001 |
| | August | 2.98 | 0.77 | <0.001 | 1.59 | 0.37 | <0.001 |
| | September | 4.12 | 0.72 | <0.001 | 5.01 | 0.59 | <0.001 |
| | Total | 3.11 | 0.76 | <0.001 | 3.00 | 0.62 | <0.001 |
| Grass, 2012 | Total | 2.28 | 0.41 | <0.001 | 3.11 | 0.38 | <0.001 |

Table 3. Summary of the posterior distribution for each parameter

| Parameter | Mean | S.D. | 2.5% | 97.5% | Rhat |
|---|---|---|---|---|---|
| $\beta_o$ | 16.55 | 3.975 | 8.393 | 23.837 | 1.006 |
| $Q_{10}$ | 2.517 | 0.115 | 2.291 | 2.752 | 1.009 |
| *a* | -1.276 | 0.476 | -1.966 | -0.312 | 1.003 |
| *b* | 0.249 | 0.111 | 0.105 | 0.483 | 1.003 |
| *c* | 2.043 | 0.573 | 1.054 | 2.956 | 1.001 |
| *d* | 3.657 | 2.816 | 0.098 | 9.460 | 1.006 |
| *k* | 4.973 | 2.900 | 0.287 | 9.722 | 1.001 |
| *r* | 0.511 | 0.289 | 0.025 | 0.976 | 1.003 |
| $\tau_{vege}$ | 0.176 | 0.126 | 0.024 | 0.501 | 1.007 |
| $\tau_{year}$ | 0.072 | 0.059 | 0.006 | 0.226 | 1.006 |
| $\tau$* | 0.225 | 0.013 | 0.199 | 0.252 | 1.001 |

* $\tau$ indicates $1/\sigma$.

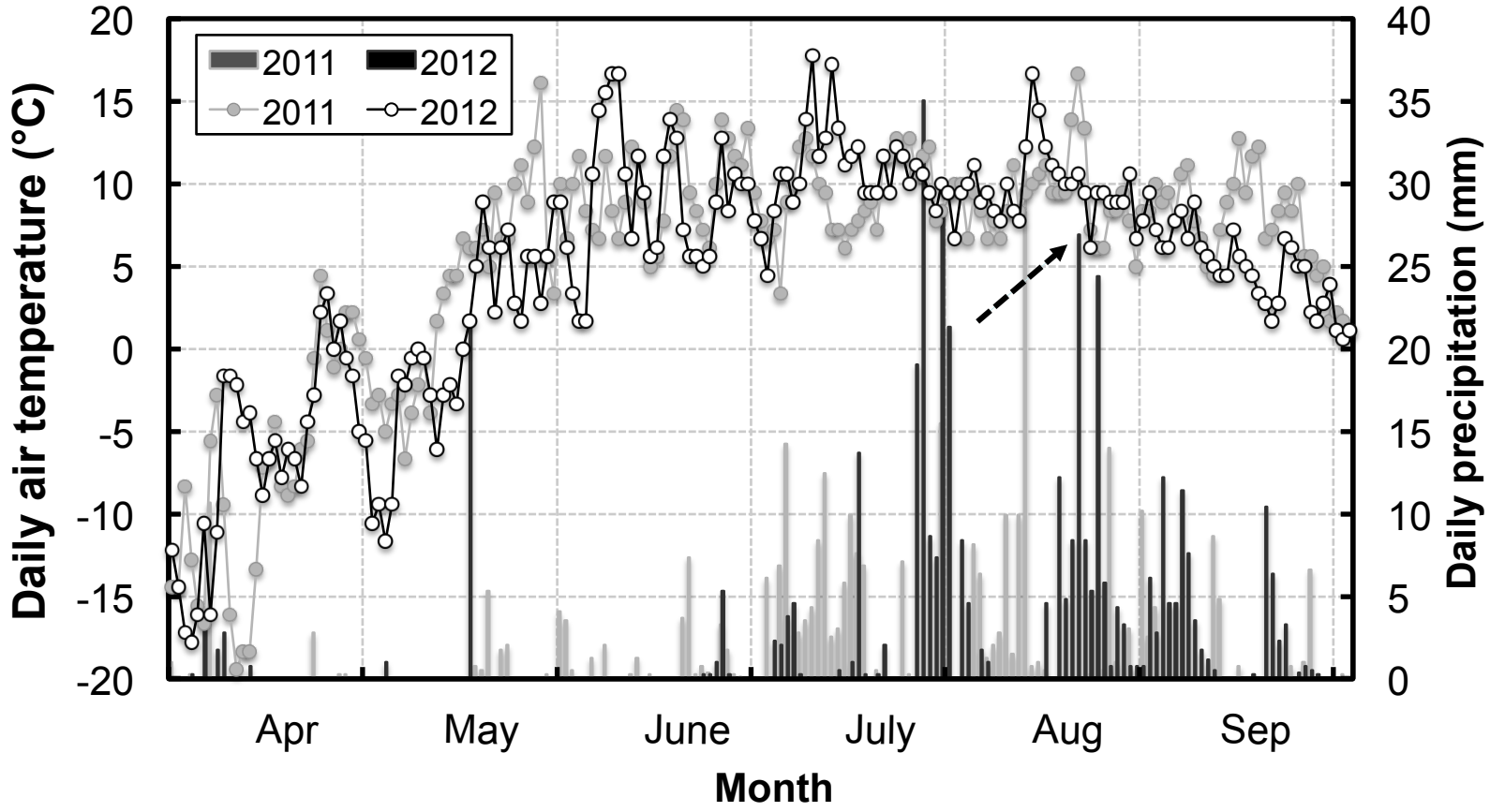
2011
2012
2011
2012
Daily air temperature (°C)
Daily precipitation (mm)
20
15
10
5
0
-5
-10
-15
-20
40
35
30
25
20
15
10
5
0
Apr
May
June
July
Aug
Sep
Month

Figure 1

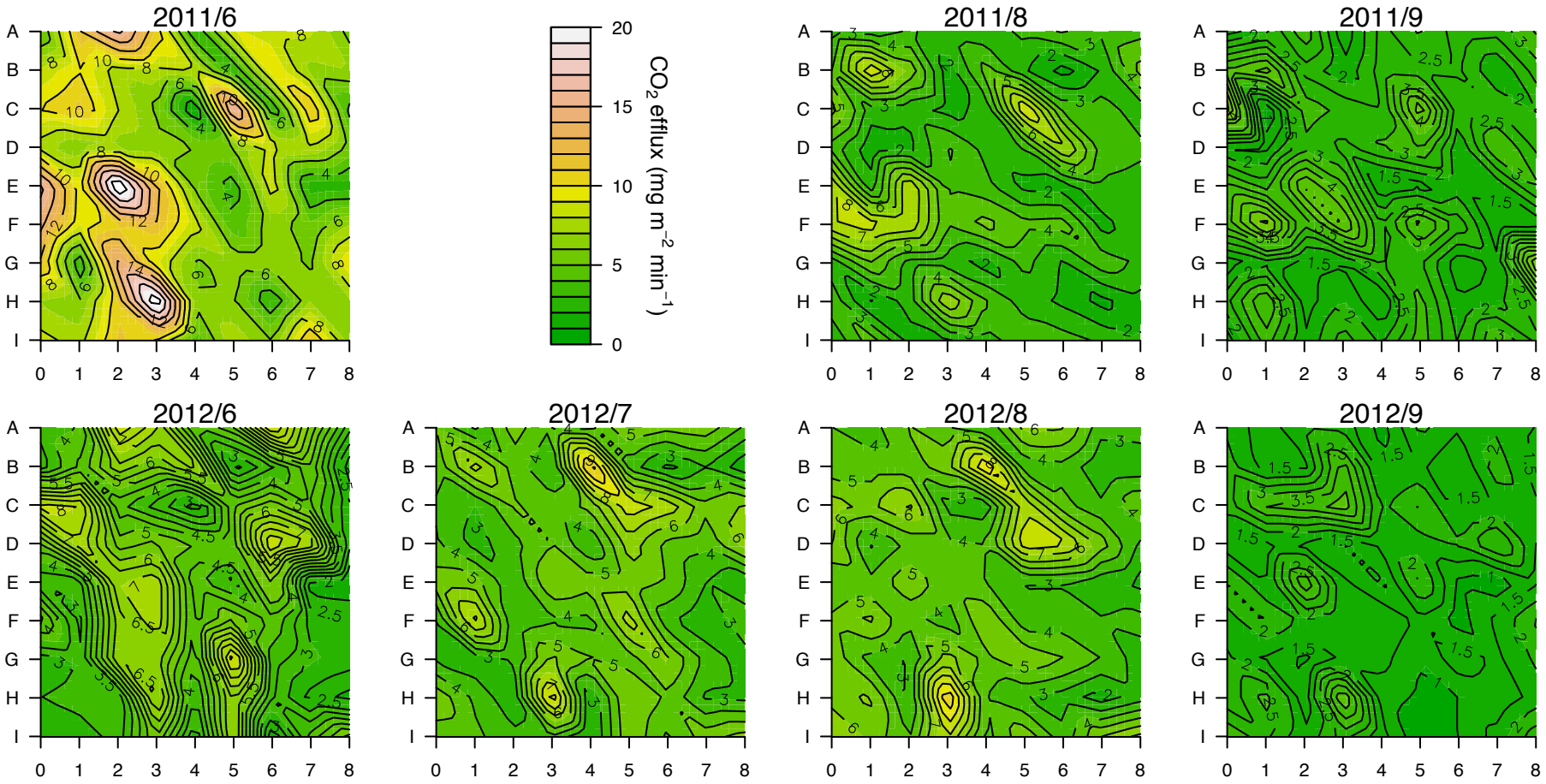
2011/6
2011/8
2011/9
2012/6
2012/7
2012/8
2012/9
CO2 efflux (mg m-2 min-1)
0
5
10
15
20
A
B
C
D
E
F
G
H
I
0 1 2 3 4 5 6 7 8

Figure 2

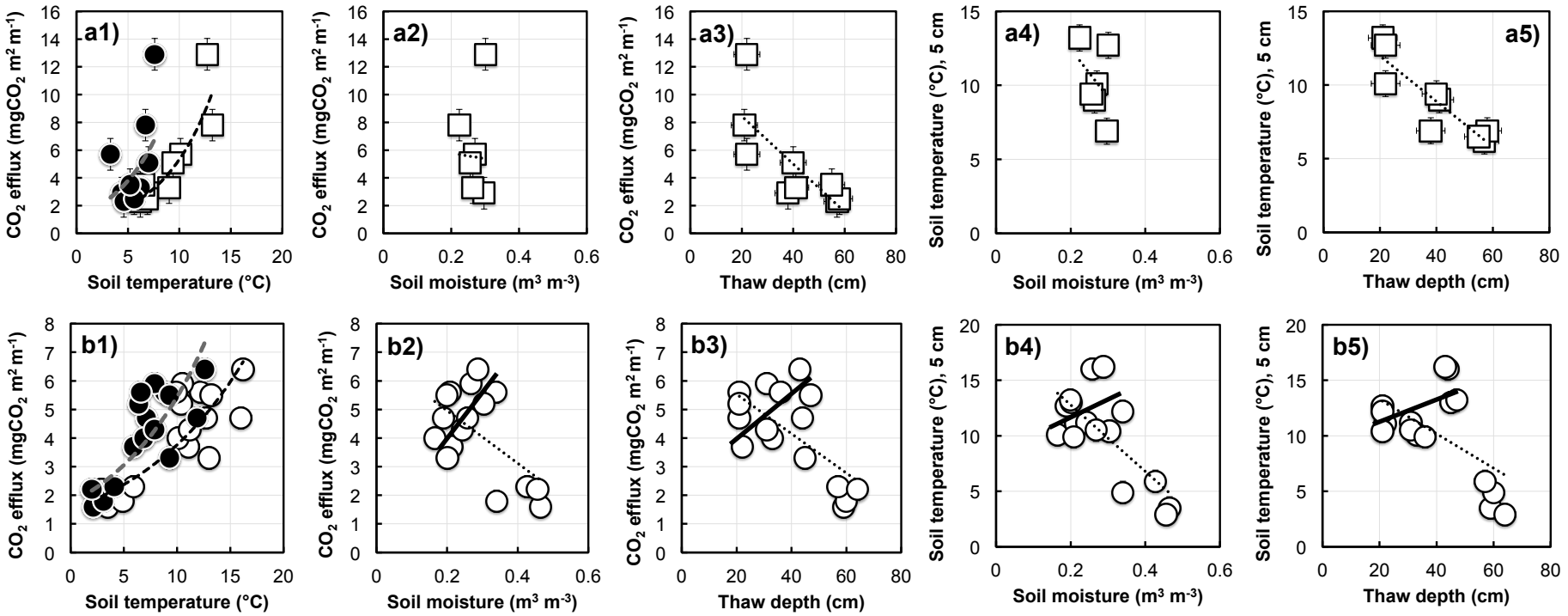
a1)
a2)
a3)
a4)
a5)
b1)
b2)
b3)
b4)
b5)
CO2 efflux (mgCO2 m2 m-1)
Soil temperature (°C)
Soil moisture (m3 m-3)
Thaw depth (cm)
Soil temperature (°C), 5 cm

Figure 3

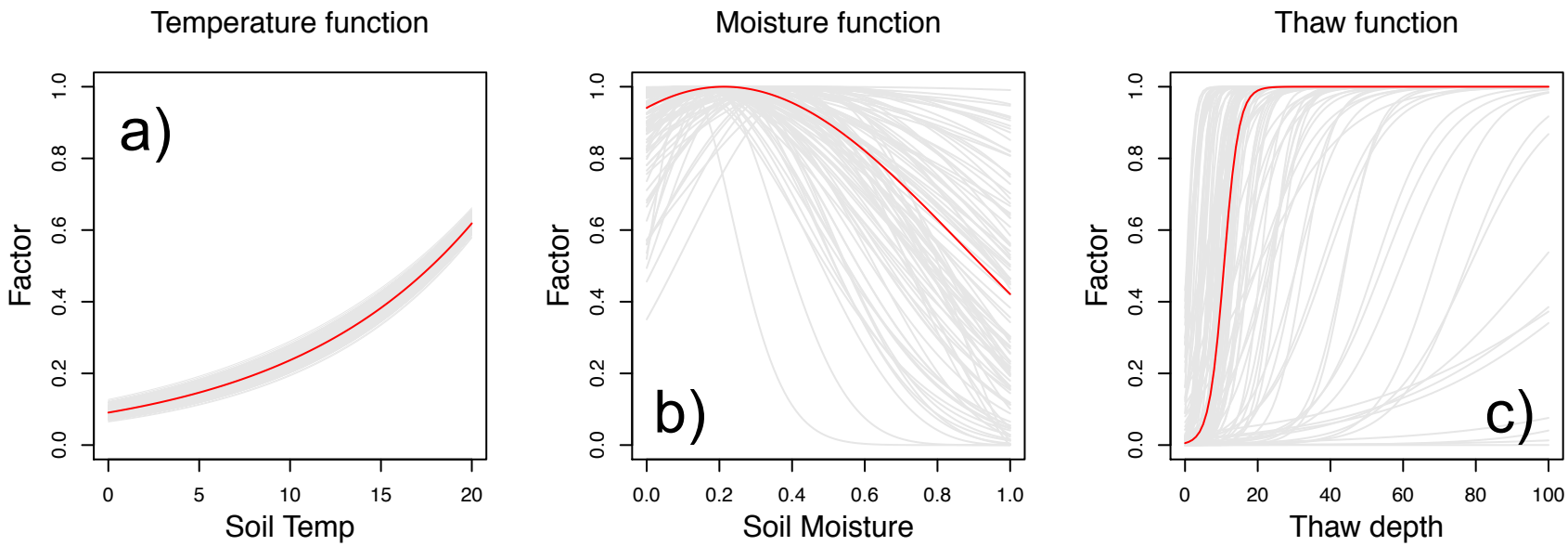
Temperature function
Moisture function
Thaw function
a)
b)
c)
Factor
Soil Temp
Soil Moisture
Thaw depth
0.0
0.2
0.4
0.6
0.8
1.0
0
5
10
15
20
40
60
80
100

Figure 4

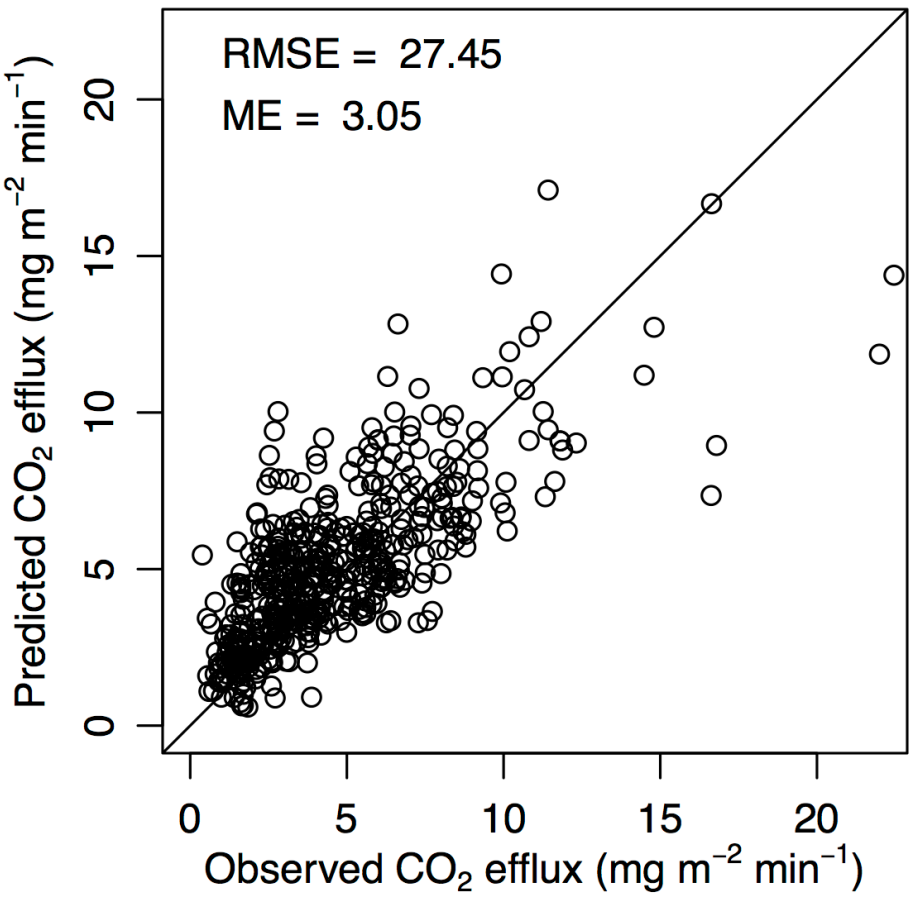
RMSE = 27.45
ME = 3.05
Predicted $CO_2$ efflux (mg $m^{-2}$ $min^{-1}$)
Observed $CO_2$ efflux (mg $m^{-2}$ $min^{-1}$)
0
5
10
15
20

Figure 5

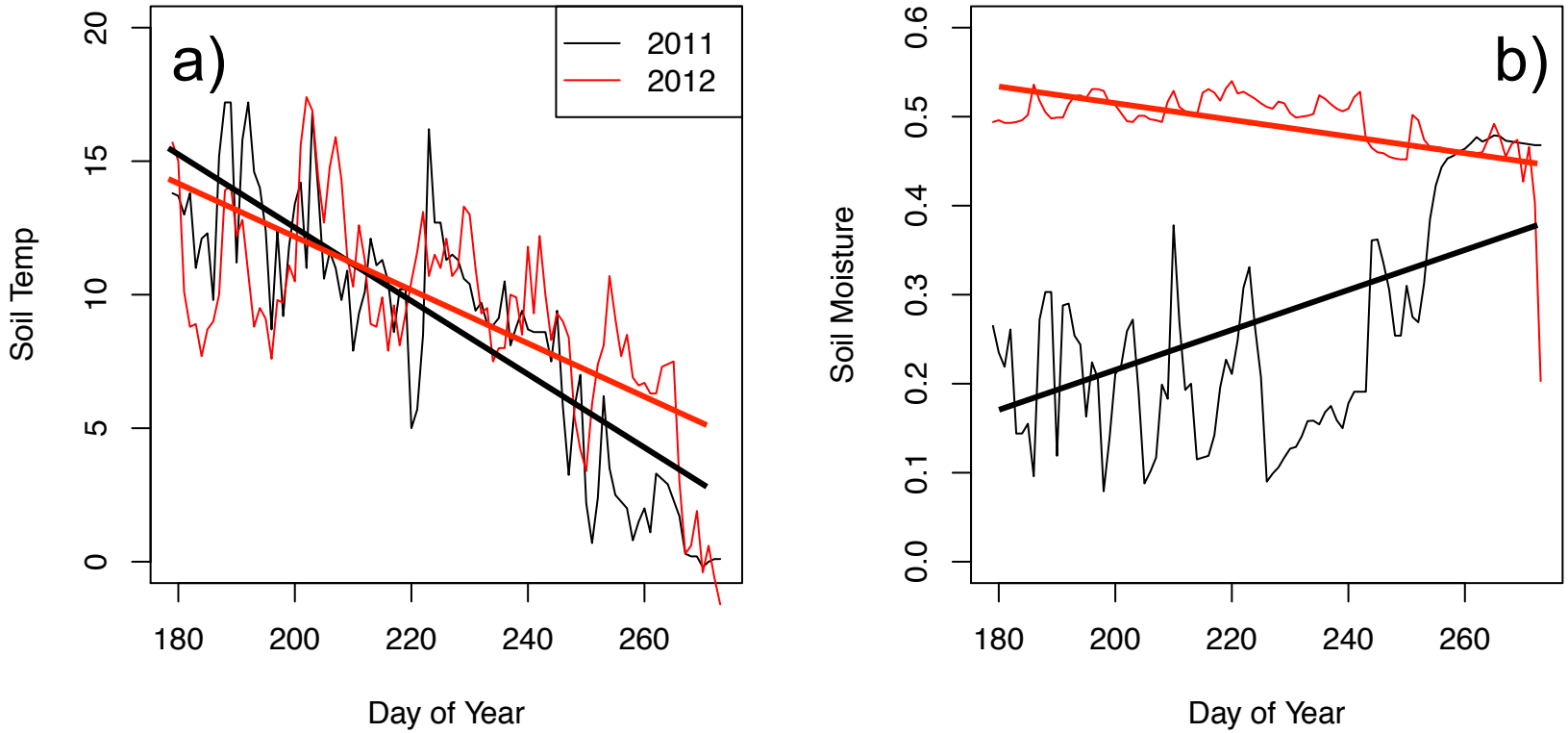
a)
2011
2012
Soil Temp
0
5
10
15
20
180
200
220
240
260
Day of Year
b)
Soil Moisture
0.0
0.1
0.2
0.3
0.4
0.5
0.6
180
200
220
240
260
Day of Year

Figure 6